

# Multilevel and Multi-index Monte Carlo methods for McKean-Vlasov equations

Abdul-Lateef Haji-Ali      Raúl Tempone

June 13, 2022

## Abstract

We address the approximation of functionals depending on a system of particles, described by stochastic differential equations (SDEs), in the mean-field limit when the number of particles approaches infinity. This problem is equivalent to estimating the weak solution of the limiting McKean-Vlasov SDE. To that end, our approach uses systems with finite numbers of particles and an Euler-Maruyama time-stepping scheme. In this case, there are two discretization parameters: the number of time steps and the number of particles. Based on these two parameters, we consider different variants of the Monte Carlo and Multilevel Monte Carlo (MLMC) methods and show that, in the best case, the optimal work complexity of MLMC to estimate the functional in one typical setting with an error tolerance of  $\text{TOL}$  is  $\mathcal{O}(\text{TOL}^{-3})$ . We also consider a method that uses the recent Multi-index Monte Carlo method and show an improved work complexity in the same typical setting of  $\mathcal{O}(\text{TOL}^{-2} \log(\text{TOL}^{-1})^2)$  when using a partitioning estimator. Our numerical experiments are carried out on the so-called Kuramoto model, a system of coupled oscillators.

**Keywords:** Multi-index Monte Carlo, Multilevel Monte Carlo, Monte Carlo, Particle systems, McKean-Vlasov, Mean-field, Stochastic Differential Equations, Weak Approximation, Sparse Approximation, Combination technique

**Class:** 65C05 (Monte Carlo methods), 65C30 (Stochastic differential and integral equations), 65C35 (Stochastic particle methods)

## 1 Introduction

In our setting, a stochastic particle system is a system of *coupled*  $d$ -dimensional stochastic differential equations (SDEs) each modeling the state of a “particle”. Such particle systems are versatile tools that can be used to model the dynamics of various complicated phenomena using relatively simple interactions, e.g., pedestrian dynamics [21, 16], collective animal behavior [10, 9] and interactions between cells [8]. One common goal of the simulation of these particle systems is to average some quantity of interest computed on *all* particles, e.g., the average velocity, average exit time or average number of particles in a specific region.

Under certain conditions, most importantly the exchangeability of particles and sufficient regularity of the SDE coefficients, the stochastic particle system approaches a mean-field limit as the number of particles tends to infinity [26]. Exchangeability of particles refers to the assumption that all permutations of the particles have the same joint distribution. If the initial states of particles are independently sampled, then all particles behave independently in the mean-field limit, due to propagation of chaos, despite the fact that the dynamics of the particles are coupled. Moreover, in the mean-field limit, each particle follows a single McKean-Vlasov SDE where the advection and/or diffusion coefficients depend on the distribution of the solution to the SDE [11]. In many cases, the objective is to approximate the expected value of a quantity of interest (QoI) in the mean-field limit as the number of particles tend to infinity, subject to some error tolerance,  $\text{TOL}$ . While it is possible to approximate the expectation of these QoIs by estimating the solution to a nonlinear PDE using traditional numerical methods, such methods usually suffer from the curse of dimensionality. Indeed, the cost of these method is usually of  $\mathcal{O}\left(\text{TOL}^{-\frac{w}{d}}\right)$  for some constant  $w > 1$  that depends on the particular numerical method. Using sparse numerical methods alleviates the curse of dimensionality but requires increasing regularity as the dimensionality of the state space

increases. On the other hand, Monte Carlo methods do not suffer from this curse with respect to the dimensionality of the state space. This work explores different variants and extensions of the Monte Carlo method when the underlying stochastic particle system satisfies certain crucial assumptions. We motivate the validity of these assumptions by verifying them numerically on a simple stochastic particle system, leaving theoretical justification to a future work.

Generally, the SDEs that constitute a stochastic particle system cannot be solved exactly and their solution must instead be approximated using the Euler-Maruyama or Milstein scheme with a number of time steps,  $N$ . This approximation parameter and a finite number of particles,  $P$ , are the two approximation parameters that are involved in approximating a finite average of the QoI computed for all particles in the system. Then, to approximate the expectation of this average, we use a Monte Carlo method. In such a method, multiple *independent* and *identical* stochastic particle systems, approximated with the same number of time steps,  $N$ , are simulated and the average QoI is computed from each and an overall average is then taken. Using this method, reducing the variance of the estimator is achieved by increasing the number of simulations of the stochastic particle system or increasing the number of particles in the system. Section 3.1 presents the Monte Carlo method more precisely in the setting of stochastic particle systems. Particle methods that are not based on Monte Carlo were also discussed in [3, 4]. In these methods, a *single* simulation of the stochastic particle system is carried out and only the number of particles is increased to reduce the variance.

As an improvement of Monte Carlo methods, the Multilevel Monte Carlo (MLMC) method was first introduced in [20] for parametric integration and in [13] for SDEs; see [14] and references therein for an overview. MLMC improves the efficiency of Monte Carlo method when only an approximation, controlled with a single discretization parameter, of the solution to the underlying system can be computed. The basic idea is to reduce the number of required samples on the finest, most accurate but most expensive discretization by reducing the variability of this approximation by using a *correlated* coarser and cheaper discretization as a control variate. More details are given in Section 3.2 for the case of stochastic particle systems. The application of MLMC to particle systems has been investigated in many works [5, 16, 25]. The same concepts have also been applied to nested expectations [14]. More recently, a particle method applying the MLMC methodology to stochastic particle systems was also introduced in [23] achieving, for a linear system with a diffusion coefficient that is independent of the state variable, a work complexity of  $\mathcal{O}(\text{TOL}^{-2}(\log(\text{TOL}^{-1}))^5)$ .

Recently, the Multi-index Monte Carlo (MIMC) method [18] was introduced to tackle high dimensional problems with more than one discretization parameter. MIMC is based on the same concepts as MLMC and improves the efficiency of MLMC even further but requires mixed regularity with respect to the discretization parameters. More details are given in Section 3.3 for the case of stochastic particle systems. In this section, we demonstrate the improved work complexity of MIMC compared with the work complexity of MC and MLMC, when applied to a stochastic particle system. More specifically, we show that, when using a naive simulation method for the particle system with quadratic complexity and an Euler-Maruyama time stepping scheme, the optimal work complexity of MIMC is  $\mathcal{O}(\text{TOL}^{-2} \log(\text{TOL}^{-1})^2)$  when the diffusion coefficient is independent of the state variable and  $\mathcal{O}(\text{TOL}^{-2} \log(\text{TOL}^{-1})^4)$  otherwise. Finally, in Section 4, we provide numerical verification for the assumptions that are made throughout the current work and the derived rates of the work complexity.

In what follows, the notation  $a \lesssim b$  means that there exists a constant  $c$  that is independent of  $a$  and  $b$  such that  $a < cb$ .

## 2 Problem Setting

Consider a system of  $P$  exchangeable stochastic differential equations (SDEs) where for  $p = 1 \dots P$ , we have the following equation for  $X_{p|P}(t) \in \mathbb{R}^d$

$$\begin{cases} dX_{p|P}(t) = \mathbb{A}(X_{p|P}(t), \lambda_P(\{X_{q|P}(t)\}_{q=1}^P)) dt + \mathbb{B}(X_{p|P}(t), \lambda_P(\{X_{q|P}(t)\}_{q=1}^P)) dW_p(t) \\ X_{p|P}(0) = x_p^0 \end{cases} \quad (1)$$

for some (possibly stochastic) functions,  $\mathbb{A} : \mathbb{R}^d \times (\mathbb{R}^d \rightarrow \mathbb{R}) \rightarrow \mathbb{R}^d$  and  $\mathbb{B} : \mathbb{R}^d \times (\mathbb{R}^d \rightarrow \mathbb{R}) \rightarrow \mathbb{R}^d \times \mathbb{R}^d$ . Here  $\mathbf{X}_P(t) \stackrel{\text{def}}{=} \{X_{p|P}(t)\}_{p=1}^P$  and

$$\lambda_P(\{X_{q|P}(t)\}_{q=1}^P)(x) \stackrel{\text{def}}{=} \frac{1}{P} \sum_{q=1}^P \delta_{X_{q|P}(t)}(x)$$

is called the empirical measure. In this setting,  $\{W_p\}_{p \geq 1}$  are mutually independent  $d$ -dimensional Wiener processes. If, moreover,  $\{x_p^0\}_{p \geq 1}$  are independent and identically distributed (i.i.d.), then under certain conditions on the smoothness and form of  $\mathbb{A}$  and  $\mathbb{B}$  [26], as  $P \rightarrow \infty$  for any  $p \in \mathbb{N}$ , the  $X_{p|\infty}$  stochastic process satisfies

$$\begin{cases} dX_{p|\infty}(t) = \mathbb{A}(X_{p|\infty}(t), \mu_\infty(t))dt + \mathbb{B}(X_{p|\infty}(t), \mu_\infty(t))dW_p(t) \\ X_{p|\infty}(0) = x_p^0, \end{cases} \quad (2)$$

where  $\mu_\infty(t) = \text{Law}(X_{p|\infty}(t))$  is the corresponding marginal law. Due to (2),  $\{X_{p|\infty}\}_p$  are i.i.d.; hence, unless we want to emphasize the particular path, we drop the  $p$ -dependence in  $X_{p|\infty}$  and refer to the random process  $X_\infty$  instead. In any case, we are interested in computing  $\mathbb{E}[\psi(X_\infty(T))]$  for some given function,  $\psi$ , and some final time,  $T$ .

**Kuramoto Example** (Fully connected Kuramoto model for synchronized oscillators). *Throughout this work, we focus on a simple, one-dimensional example of (1). For  $p = 1, 2, \dots, P$ , we seek  $X_{p|P}(t) \in \mathbb{R}$  that satisfies*

$$\begin{aligned} dX_{p|P}(t) &= \left( \vartheta_p + \frac{1}{P} \sum_{q=1}^P \sin(X_{p|P}(t) - X_{q|P}(t)) \right) dt + \sigma dW_p(t) \\ X_{p|P}(0) &= x_p^0, \end{aligned} \quad (3)$$

where  $\{\vartheta_p\}_p$  are i.i.d. and independent from the set of i.i.d. random variables  $\{x_p^0\}_p$  and the Wiener processes  $\{W_p\}_p$ . We are interested in

$$\text{Total disorder} = (\mathbb{E}[\cos(X_\infty(T))])^2 + (\mathbb{E}[\sin(X_\infty(T))])^2,$$

a real number between zero and one that measures the level of synchronization in the system with an infinite number of oscillators [1]. In this case, we need two estimators: one where we take  $\psi(\cdot) = \sin(\cdot)$  and the other where we take  $\psi(\cdot) = \cos(\cdot)$ .

While it is computationally efficient to approximate  $\mathbb{E}[\psi(X_\infty(T))]$  by solving the integro-differential Fokker-Planck PDE of  $\mu_\infty$  when the state dimensionality,  $d$ , is small (cf., e.g., [16]), the cost of a standard full tensor approximation increases exponentially as the dimensionality of the state space increases. On the other hand, using sparse approximation techniques to solve the PDE requires increasing regularity assumptions as the dimensionality of the state space increases. Instead, in this work, we focus on approximating the value of  $\mathbb{E}[\psi(X_\infty)]$  by simulating the SDE system in (1). Let us now define

$$\phi_P \stackrel{\text{def}}{=} \frac{1}{P} \sum_{p=1}^P \psi(X_{p|P}(T)). \quad (4)$$

Here, due to exchangeability,  $\{X_{p|P}(T)\}_{p=1}^P$  are identically distributed but they are not independent since they are taken from the same realization of the particle system. Nevertheless, we have  $\mathbb{E}[\phi_P] = \mathbb{E}[\psi(X_{p|P}(T))]$  for any  $p$  and  $P$ . Moreover, we can show that  $\phi_P \xrightarrow{L^2} \mathbb{E}[\psi(X_\infty(T))]$  using the results in [26] for a class of stochastic particle systems with constant diffusion coefficients. In this case, with respect to the number of particles,  $P$ , the cost of a naive calculation of  $\phi_P$  is  $\mathcal{O}(P^2)$  due to the linear sum in (1) for every particle in the system. It is possible to take  $\{X_{p|P}\}_{p=1}^P$  in (4) as i.i.d., i.e., for each  $p = 1 \dots P$ ,  $X_{p|P}$  is taken from a different independent realization of the system (1). In this case, the usual law of large numbers applies, but the cost of a naive calculation of  $\phi_P$  is  $\mathcal{O}(P^3)$ . For this reason, we focus in this work on the former method of taking identically distributed but not independent  $\{X_{p|P}\}_{p=1}^P$ .

Following the setup in [7, 19], our objective is to build a random estimator,  $\mathcal{A}$ , approximating  $\phi_\infty \stackrel{\text{def}}{=} \mathbb{E}[\psi(X_\infty(T))]$  with minimal work, i.e., we wish to satisfy the constraint

$$\mathbb{P}[|\mathcal{A} - \phi_\infty| \geq \text{TOL}] \leq \epsilon$$

for a given error tolerance, TOL, and a given confidence level determined by  $0 < \epsilon \ll 1$ . We instead impose the following, more restrictive, two constraints:

$$\begin{aligned} \textbf{Bias constraint:} \quad & \mathbb{E}[\mathcal{A} - \phi_\infty] \leq (1 - \theta)\text{TOL}, \\ \textbf{Statistical constraint:} \quad & \mathbb{P}[|\mathcal{A} - \mathbb{E}[\mathcal{A}]| \geq \theta\text{TOL}] \leq \epsilon, \end{aligned} \quad (5)$$

for a given tolerance splitting parameter,  $\theta \in (0, 1)$ , possibly a function of TOL. Assuming (at least asymptotic) normality of the estimator,  $\mathcal{A}$ , we replace the statistical constraint by a constraint on the variance and write:

$$\textbf{Variance constraint:} \quad \text{Var}[\mathcal{A}] \leq \left( \frac{\theta\text{TOL}}{C_\epsilon} \right)^2. \quad (6)$$

Here,  $0 < C_\epsilon$  is such that  $\Phi(C_\epsilon) = 1 - \frac{\epsilon}{2}$ , where  $\Phi$  is the cumulative distribution function of a standard normal random variable. The asymptotic normality of the estimator is usually shown using some form of the Central Limit Theorem (CLT) or the Lindeberg-Feller theorem (See, e.g., [7, 18] for CLT results for the MLMC and MIMC estimators and Figure 3-right).

As previously mentioned, we wish to approximate the values of  $X_\infty$  by using (1) with a finite number of particles,  $P$ . For a given number of particles,  $P$ , a solution to (1) is not readily available. Instead, we have to discretize the system of SDEs using, for example, the Euler-Maruyama time-stepping scheme with  $N$  time steps. For  $n = 0, 1, 2, \dots, N-1$ ,

$$\begin{aligned} X_{p|P}^{n+1|N} - X_{p|P}^{n|N} &= \mathbb{A} \left( X_{p|P}^{n|N}, \lambda_P \left( \mathbf{X}_P^{n|N} \right) \right) \frac{T}{N} + \mathbb{B} \left( X_{p|P}^{n|N}, \lambda_P \left( \mathbf{X}_P^{n|N} \right) \right) \Delta W_p^{n|N} \\ X_{p|P}^{0|N} &= x_p^0, \end{aligned}$$

where  $\Delta W_p^{n|N} \sim \mathcal{N} \left( 0, \frac{T}{N} \right)$  are i.i.d. For the remainder of this work, we use the notation

$$\phi_P^N \stackrel{\text{def}}{=} \frac{1}{P} \sum_{p=1}^P \psi \left( X_{p|P}^{N|N} \right).$$

At this point, we make the following assumptions:

$$\left| \mathbb{E}[\phi_P^N - \psi(X_\infty)] \right| \leq \left| \mathbb{E}[\psi(X_{\cdot|P}^{N|N}) - \psi(X_{\cdot|P})] \right| + \left| \mathbb{E}[\psi(X_{\cdot|P}) - \psi(X_\infty)] \right| \lesssim N^{-1} + P^{-1}, \quad (\textbf{P1})$$

$$\text{Var}[\phi_P^N] \lesssim P^{-1}. \quad (\textbf{P2})$$

The first assumption (P1) relates to weak convergence. Indeed, the weak convergence of the Euler-Maruyama method with respect to the number of time steps is a standard result shown, for example, in [22] by assuming 4-time differentiability of  $\mathbb{A}$  and  $\mathbb{B}$ . Showing that the constant multiplying  $N^{-1}$  is bounded for all  $P$  is straightforward by extending the standard proof of weak convergence the Euler-Maruyama method in [22, Chapter 14] and assuming boundedness of  $\mathbb{A}$  and  $\mathbb{B}$ . On the other hand, the weak convergence with respect to the number of particles and Assumption (P2) will be verified numerically later. In general these assumptions also translate to smoothness and boundedness assumptions on  $\mathbb{A}$  and  $\mathbb{B}$ .

Finally, we remark that, with a naive method, the total cost to compute a single sample of  $\phi_P^N$  is  $\mathcal{O}(NP^2)$ . The quadratic power of  $P$  can be reduced by using, for example, a multipole algorithm. In general, we consider the work required to compute one sample of  $\phi_P^N$  as  $\mathcal{O}(NP^{\hat{\gamma}})$  for a positive constant,  $\hat{\gamma} \geq 1$ .

### 3 Monte Carlo methods

In this section we study different Monte Carlo methods that can be used to estimate the previous quantity,  $\phi_\infty$ . In the following, we use the notation  $\omega_{p:P}^m \stackrel{\text{def}}{=} (\omega_q^m)_{q=p}^P$  where, for each  $q$ ,  $\omega_q^m$  denotes

the  $m$ 'th sample of the set of underlying random variables that are used in calculating  $X_{q|P}^{N|N}$ , i.e., the Wiener path,  $W_q$ , the initial condition,  $x_q^0$ , and any random variables that are used in  $\mathbb{A}$  or  $\mathbb{B}$ . Moreover, we sometimes write  $\phi_P^N(\omega_{1:P}^m)$  to emphasize the dependence of the  $m$ 'th sample of  $\phi_P^N$  on the underlying random variables.

### 3.1 Monte Carlo (MC)

The first estimator that we look at is a Monte Carlo estimator. For a given number of samples,  $M$ , number of particles,  $P$ , and number of time steps,  $N$ , we can write the MC estimator as follows:

$$\mathcal{A}_{\text{MC}}(M, P, N) = \frac{1}{M} \sum_{m=1}^M \phi_P^N(\omega_{1:P}^m).$$

Here,

$$\mathbb{E}[\mathcal{A}_{\text{MC}}(M, P, N)] = \mathbb{E}[\phi_P^N] = \frac{1}{P} \sum_{p=1}^P \mathbb{E}[\psi(X_{p|P}^{N|N})] = \mathbb{E}[\psi(X_{\cdot|P}^{N|N})],$$

$$\text{and } \text{Var}[\mathcal{A}_{\text{MC}}(M, P, N)] = \frac{\text{Var}[\phi_P^N]}{M},$$

while the total work is  $\text{Work}[\mathcal{A}_{\text{MC}}(M, P, N)] = MP^{\hat{\gamma}}N$ .

Hence, due to **(P1)**, we must have  $P = \mathcal{O}(\text{TOL}^{-1})$  and  $N = \mathcal{O}(\text{TOL}^{-1})$  to satisfy (5), and, due to **(P2)**, we must have  $M = \mathcal{O}(\text{TOL}^{-1})$  to satisfy (6). Based on these choices, the total work to compute  $\mathcal{A}_{\text{MC}}$  is

$$\text{Work}[\mathcal{A}_{\text{MC}}] = \mathcal{O}(\text{TOL}^{-2-\hat{\gamma}}).$$

**Kuramoto Example.** Using a naive calculation method of  $\phi_P^N$  (i.e.,  $\hat{\gamma} = 2$ ) gives a work complexity of  $\mathcal{O}(\text{TOL}^{-4})$ . See also Table 1 for the work complexities for different common values of  $\hat{\gamma}$ .

### 3.2 Multilevel Monte Carlo (MLMC)

For a given  $L \in \mathbb{N}$ , define two hierarchies,  $\{N_\ell\}_{\ell=0}^L$  and  $\{P_\ell\}_{\ell=0}^L$ , satisfying  $P_{\ell-1} \leq P_\ell$  and  $N_{\ell-1} \leq N_\ell$  for all  $\ell$ . Then, we can write the MLMC estimator as follows:

$$\mathcal{A}_{\text{MLMC}}(L) = \sum_{\ell=0}^L \frac{1}{M_\ell} \sum_{m=1}^{M_\ell} \left( \phi_{P_\ell}^{N_\ell} - \phi_{P_{\ell-1}}^{N_{\ell-1}} \right) \left( \omega_{1:P_\ell}^{(\ell,m)} \right), \quad (7)$$

where we later choose the function  $\varphi_{P_{\ell-1}}^{N_{\ell-1}}(\cdot)$  such that  $\varphi_{P_{\ell-1}}^{N_{\ell-1}}(\cdot) = 0$  and  $\mathbb{E}[\varphi_{P_{\ell-1}}^{N_{\ell-1}}] = \mathbb{E}[\phi_{P_{\ell-1}}^{N_{\ell-1}}]$ , so that  $\mathbb{E}[\mathcal{A}_{\text{MLMC}}] = \mathbb{E}[\phi_{P_L}^{N_L}]$  due to the telescopic sum. For MLMC to have better work complexity than that of Monte Carlo,  $\phi_{P_\ell}^{N_\ell}(\omega_{1:P_\ell}^{(\ell,m)})$  and  $\varphi_{P_{\ell-1}}^{N_{\ell-1}}(\omega_{1:P_\ell}^{(\ell,m)})$  must be correlated for every  $\ell$  and  $m$ , so that their difference has a smaller variance than either  $\phi_{P_\ell}^{N_\ell}(\omega_{1:P_\ell}^{(\ell,m)})$  or  $\varphi_{P_{\ell-1}}^{N_{\ell-1}}(\omega_{1:P_\ell}^{(\ell,m)})$  for all  $\ell > 0$ .

Given two discretization levels,  $N_\ell$  and  $N_{\ell-1}$ , with the same number of particles,  $P$ , we can generate a sample of  $\varphi_P^{N_{\ell-1}}(\omega_{1:P}^{(\ell,m)})$  that is correlated to  $\phi_P^{N_\ell}(\omega_{1:P}^{(\ell,m)})$  by taking

$$\varphi_P^{N_{\ell-1}}(\omega_{1:P}^{(\ell,m)}) = \phi_P^{N_{\ell-1}}(\omega_{1:P}^{(\ell,m)}).$$

That is, we use the same samples of the initial values,  $\{x_p^0\}_{p \geq 1}$ , the same Wiener paths,  $\{W_p\}_{p=1}^P$ , discretized with  $N_{\ell-1}$  steps, and, in case they are random as in (3), the same samples of the advection and diffusion coefficients,  $\mathbb{A}$  and  $\mathbb{B}$ , respectively. In case the diffusion coefficient,  $\mathbb{B}$ , is not a constant, we can improve the correlation by using an antithetic sampler as detailed in [15] or by using a higher-order scheme like the Milstein scheme [12]. In the Kuramoto example, the Euler-Maruyama and the Milstein schemes are equivalent because the diffusion is constant.

On the other hand, given two different sizes of the particle system,  $P_\ell$  and  $P_{\ell-1}$ , with the same discretization level,  $N$ , we can generate a sample of  $\varphi_{P_{\ell-1}}^N(\omega_{1:P_\ell}^{(\ell,m)})$  that is correlated to  $\phi_{P_\ell}^N(\omega_{1:P_\ell}^{(\ell,m)})$  by taking

$$\varphi_{P_{\ell-1}}^N(\omega_{1:P_\ell}^{(\ell,m)}) = \bar{\varphi}_{P_{\ell-1}}^N(\omega_{1:P_\ell}^{(\ell,m)}) \stackrel{\text{def}}{=} \phi_{P_{\ell-1}}^N\left(\omega_{1:P_{\ell-1}}^{(\ell,m)}\right). \quad (8)$$

In other words, we use the same  $P_{\ell-1}$  noise paths out of the total  $P_\ell$  noise paths to run an independent simulation of the stochastic system with  $P_{\ell-1}$  particles.

We also consider another estimator that is more correlated with  $\phi_{P_\ell}^N(\omega_{1:P_\ell}^{(\ell,m)})$ . The “antithetic” estimator was first independently introduced in [16, Chapter 5] and [5] and subsequently used in other works on particle systems [25] and nested simulations [14]. In this work, we call this estimator a “partitioning” estimator to clearly distinguish it from the antithetic estimator in [15]. We assume that  $P_\ell = \hat{\beta}P_{\ell-1}$  for all  $\ell$  and some positive integer  $\hat{\beta}$  and take

$$\varphi_{P_{\ell-1}}^N(\omega_{1:P_\ell}^{(\ell,m)}) = \hat{\varphi}_{P_{\ell-1}}^N(\omega_{1:P_\ell}^{(\ell,m)}) \stackrel{\text{def}}{=} \frac{1}{\hat{\beta}} \sum_{i=1}^{\hat{\beta}} \phi_{P_{\ell-1}}^N\left(\omega_{((i-1)P_{\ell-1}+1):iP_{\ell-1}}^{(\ell,m)}\right). \quad (9)$$

That is, we split the underlying  $P_\ell$  sets of random variables into  $\hat{\beta}$  identically distributed and independent groups, each of size  $P_{\ell-1}$ , and independently simulate  $\hat{\beta}$  particle systems, each of size  $P_{\ell-1}$ . Finally, for each particle system, we compute the quantity of interest and take the average of the  $\hat{\beta}$  quantities.

In the following subsections, we look at different settings in which either  $P_\ell$  or  $N_\ell$  depends on  $\ell$  while the other parameter is constant for all  $\ell$ . We begin by recalling the optimal convergence rates of MLMC when applied to a generic random process,  $Y$ , with a trivial generalization to the case when there are two discretization parameters: One that is a function of the level,  $\ell$ , and the other,  $\mathcal{L}$ , that is fixed for all levels.

**Theorem 3.1** (Optimal MLMC complexity). *Let  $Y_{\mathcal{L},\ell}$  be an approximation of  $Y$  for every  $(\mathcal{L}, \ell) \in \mathbb{N}^2$ . Consider the MLMC estimator*

$$\mathcal{A}_{\text{MLMC}}(L, \mathcal{L}) = \sum_{\ell=0}^L \frac{1}{M_\ell} \sum_{m=1}^{M_\ell} (Y_{\mathcal{L},\ell} - Y_{\mathcal{L},\ell-1})$$

with  $Y_{\mathcal{L},-1} = 0$  and for  $w, \gamma, s, \tilde{w}, \tilde{\gamma}, \tilde{c} > 0$  where  $\tilde{c} \leq \frac{\tilde{w}}{\tilde{\gamma}}$  and  $s \leq 2w$ , assume the following

1.  $|\mathbb{E}[Y - Y_{\mathcal{L},\ell}]| \lesssim \exp(-\tilde{w}\mathcal{L}) + \exp(-w\ell)$
2.  $\text{Var}[Y_{\mathcal{L},\ell} - Y_{\mathcal{L},\ell-1}] \lesssim \exp(-\tilde{c}\mathcal{L}) \exp(-s\ell)$
3.  $\text{Work}[Y_{\mathcal{L},\ell} - Y_{\mathcal{L},\ell-1}] \lesssim \exp(\tilde{\gamma}\mathcal{L}) \exp(\gamma\ell)$ .

Then, for any  $\text{TOL} < e^{-1}$ , there exists  $L, \mathcal{L}$  and a sequence of  $\{M_\ell\}_{\ell=0}^L$  such that (5) and (6) are satisfied and

$$\text{Work}[\mathcal{A}_{\text{MLMC}}] \lesssim \begin{cases} \text{TOL}^{-2-(\frac{\tilde{\gamma}}{w}-\tilde{c})} & \text{if } s > \gamma \\ \text{TOL}^{-2-(\frac{\tilde{\gamma}}{w}-\tilde{c})} \log(\text{TOL}^{-1})^2 & \text{if } s = \gamma \\ \text{TOL}^{-2-(\frac{\tilde{\gamma}}{w}-\tilde{c})-\frac{\gamma-\tilde{s}}{w}} & \text{if } s < \gamma. \end{cases} \quad (10)$$

*Proof.* Straightforward derivation from the proof of [6, Theorem 1].  $\square$

### 3.2.1 MLMC hierarchy based on the number of time steps

In this setting, we take  $N_\ell = \bar{\beta}^\ell$  for some  $\bar{\beta} > 0$  and  $P_\ell = P_L$  for all  $\ell$ , i.e., the number of particles is a constant,  $P_L$ , on all levels. We make an extra assumption in this case, namely:

$$\text{Var}\left[\phi_{P_L}^{N_\ell} - \varphi_{P_L}^{N_{\ell-1}}\right] \lesssim P_L^{-1} N_\ell^{-\bar{s}} = P_L^{-1} (\bar{\beta})^{-\bar{s}\ell}. \quad (\text{MLMC1})$$

The factor  $(\bar{\beta})^{-\bar{s}\ell}$  is the usual assumption on the variance convergence of the level difference in MLMC theory [13] and is a standard result for the Euler-Maruyama scheme [22]. On the other



hand, the factor  $P_L^{-1}$  can be motivated from (P2), which states that the variance of each term in the difference converges at this rate.

Due to Theorem 3.1, we can conclude that the work complexity of MLMC is

$$\text{Work}[\mathcal{A}_{\text{MLMC}}] \lesssim \begin{cases} \text{TOL}^{-1-\hat{\gamma}} & \text{if } \bar{s} > 1 \\ \text{TOL}^{-1-\hat{\gamma}} \log(\text{TOL}^{-1})^2 & \text{if } \bar{s} = 1 \\ \text{TOL}^{-2-\hat{\gamma}+\bar{s}} & \text{if } \bar{s} < 1. \end{cases} \quad (11)$$

**Kuramoto Example.** In this example, since the diffusion coefficient is constant, we have  $\bar{s} = 2$  (see Figure 1), and a naive calculation method of  $\phi_P^N$  ( $\hat{\gamma} = 2$ ) gives a work complexity of  $\mathcal{O}(\text{TOL}^{-3})$ . See also Table 1 for the work complexities for different common values of  $\bar{s}$  and  $\hat{\gamma}$ .

### 3.2.2 MLMC hierarchy based on the number of particles

In this setting, we take  $P_\ell = \hat{\beta}^\ell$  for some  $\hat{\beta} > 0$  and  $N_\ell = N_L$  for all  $\ell$ , i.e., we take the number of time steps to be a constant,  $N_L$ , on all levels. We make an extra assumption in this case:

$$\text{Var}[\phi_{P_\ell}^{N_L} - \varphi_{P_{\ell-1}}^{N_L}] \lesssim P_\ell^{-\hat{s}-1} = \hat{\beta}^{-\ell(\hat{s}+1)}, \quad (\text{MLMC2})$$

for some constant  $\hat{s} \geq 0$ . The factor  $\hat{\beta}^{-\hat{s}\ell}$  is the usual assumption on the variance convergence of the level difference in MLMC theory [13] and is shown in, e.g., [2] for a certain class of particle systems. On the other hand, the factor  $P_\ell^{-1}$  can be motivated from (P2), since the variance of each term in the difference is converging at this rate.

Due to Theorem 3.1, we can conclude that the work complexity of MLMC in this case is

$$\text{Work}[\mathcal{A}_{\text{MLMC}}] \lesssim \begin{cases} \text{TOL}^{-3} & \text{if } \hat{s} + 1 > \hat{\gamma} \\ \text{TOL}^{-3} \log(\text{TOL}^{-1})^2 & \text{if } \hat{s} + 1 = \hat{\gamma} \\ \text{TOL}^{-2-\hat{\gamma}+\hat{s}} & \text{if } \hat{s} + 1 < \hat{\gamma}. \end{cases} \quad (12)$$

**Kuramoto Example.** Using a naive calculation method of  $\phi_P^N$  ( $\hat{\gamma} = 2$ ), we distinguish between the two samplers:

- Using the sampler  $\bar{\phi}$  in (8), we verify numerically that  $\hat{s} = 0$  (cf. Figure 1). Hence, the work complexity is  $\mathcal{O}(\text{TOL}^{-4})$ , which is the same work complexity as a Monte Carlo estimator. This should be expected since using the “correlated” samples of  $\bar{\varphi}_{P_{\ell-1}}^N$  and  $\phi_{P_\ell}^N$  do not reduce the variance of the difference, as Figure 1 shows.
- Using the partitioning estimator,  $\hat{\phi}$ , in (9), we have  $\hat{s} = 1$  (See Figure 1). Hence, the work complexity is  $\mathcal{O}(\text{TOL}^{-3} \log(\text{TOL}^{-1})^2)$ . Here the samples of  $\hat{\varphi}_{P_{\ell-1}}^N$  have higher correlation to corresponding samples of  $\phi_{P_\ell}^N$ , thus reducing the variance of the difference. Still, using MLMC with hierarchies based on the number of time steps (fixing the number of particles) yields better work complexity. See also Table 1 for the work complexities for different common values of  $\bar{s}$  and  $\hat{\gamma}$ .

### 3.2.3 MLMC hierarchy based on both the number of particles and the number of times steps

In this case, we vary both the number of particles and the number of time steps across MLMC levels. That is, we take  $P_\ell = \hat{\beta}^\ell$  and  $N_\ell = \bar{\beta}^\ell$  for all  $\ell$ . In this case, a reasonable assumption is

$$\text{Var}[\phi_{P_\ell}^{N_\ell} - \phi_{P_{\ell-1}}^{N_{\ell-1}}] \lesssim \hat{\beta}^{-\ell} \left( \max(\hat{\beta}^{-\hat{s}}, \bar{\beta}^{-\bar{s}}) \right)^\ell. \quad (\text{MLMC3})$$

The factor  $\hat{\beta}^{-\ell}$  can be motivated from (P2) since the variance of each term in the difference is converges at this rate. On the other hand,  $\left( \max(\hat{\beta}^{-\hat{s}}, \bar{\beta}^{-\bar{s}}) \right)^\ell$  is the slower convergence of (MLMC1) and (MLMC2).

Due to Theorem 3.1 and defining

$$\begin{aligned} s &= \log(\widehat{\beta}) + \min(\widehat{s} \log(\widehat{\beta}), \bar{s} \log(\bar{\beta})) \\ \gamma &= \widehat{\gamma} \log(\widehat{\beta}) + \log(\bar{\beta}) \\ w &= \min(\log(\widehat{\beta}), \log(\bar{\beta})), \end{aligned}$$

we can conclude that the work complexity of MLMC is

$$\text{Work}[\mathcal{A}_{\text{MLMC}}] \lesssim \begin{cases} \text{TOL}^{-2} & \text{if } s > \gamma \\ \text{TOL}^{-2} \log(\text{TOL}^{-1})^2 & \text{if } s = \gamma \\ \text{TOL}^{-2 - \frac{\gamma-s}{w}} & \text{if } s < \gamma. \end{cases} \quad (13)$$

**Kuramoto Example.** We choose  $\widehat{\beta} = \bar{\beta}$  and use a naive calculation method of  $\phi_P^N$  (yielding  $\widehat{\gamma} = 2$ ) and the partitioning sampler (yielding  $\widehat{s} = 1$ ). Finally the constant diffusion coefficient gives  $\bar{s} = 2$ . Refer to Figure 1 for numerical verification. Based on these rates, we have  $s = 2 \log(\widehat{\beta})$ ,  $w = \log(\widehat{\beta})$  and  $\gamma = 3 \log(\widehat{\beta})$ . The MLMC work complexity in this case is  $\mathcal{O}(\text{TOL}^{-3})$ . See also Table 1 for the work complexities for different common values of  $\bar{s}$  and  $\widehat{\gamma}$ .

### 3.3 Multi-index Monte Carlo (MIMC)

Following [18], for every  $\alpha = (\alpha_1, \alpha_2) \in \mathbb{N}^2$ , let  $P_{\alpha_1} = \widehat{\beta}^{\alpha_1}$  and  $N_{\alpha_2} = \bar{\beta}^{\alpha_2}$  and define the first-order mixed-difference operator in two dimensions as

$$\Delta \phi_{P_{\alpha_1}}^{N_{\alpha_2}} = \left( \phi_{P_{\alpha_1}}^{N_{\alpha_2}} - \phi_{P_{\alpha_1-1}}^{N_{\alpha_2}} \right) - \left( \phi_{P_{\alpha_1}}^{N_{\alpha_2-1}} - \phi_{P_{\alpha_1-1}}^{N_{\alpha_2-1}} \right)$$

with  $\phi_{P_{-1}}^N = 0$  and  $\phi_P^{N_{-1}} = 0$ . The MIMC estimator is then written for a given  $\mathcal{I} \in \mathbb{N}^2$  as

$$\mathcal{A}_{\text{MIMC}} = \sum_{\alpha \in \mathcal{I}} \frac{1}{M_{\alpha}} \sum_{m=1}^{M_{\alpha}} \Delta \phi_{P_{\alpha_1}}^{N_{\alpha_2}} \quad (14)$$

At this point, similar to the original work on MIMC [18], we make the following assumptions on the convergence and cost of  $\Delta \phi_{P_{\alpha_1}}^{N_{\alpha_2}}$ , namely

$$\mathbb{E} \left[ \Delta \phi_{P_{\alpha_1}}^{N_{\alpha_2}} \right] \lesssim P_{\alpha_1}^{-1} N_{\alpha_2}^{-1} \quad (\text{MIMC1})$$

$$\text{Var} \left[ \Delta \phi_{P_{\alpha_1}}^{N_{\alpha_2}} \right] \lesssim P_{\alpha_1}^{-\widehat{s}-1} N_{\alpha_2}^{-\bar{s}}. \quad (\text{MIMC2})$$

Assumption (MIMC1) is motivated from (P1) by assuming that the mixed first order difference,  $\Delta \phi_{P_{\alpha_1}}^{N_{\alpha_2}}$ , gives a product of the convergence terms instead of a sum. Similarly, (MIMC2) is motivated from (MLMC1) and (MLMC2). To the best of our knowledge, there are currently no proofs of these assumptions for particle systems, but we verify them numerically for (3) in Figure 2.

Henceforth, we will assume that  $\bar{\beta} = \widehat{\beta}$  for easier presentation. Following [18, Lemma 2.1] and recalling the assumption on cost per sample,  $\text{Work} \left[ \Delta \phi_{P_{\alpha_1}}^{N_{\alpha_2}} \right] \lesssim P_{\alpha_1}^{\widehat{\gamma}} N_{\alpha_2}$ , then, for every value of  $L \in \mathbb{R}^+$ , the optimal set can be written as

$$\mathcal{I}(L) = \{ \alpha \in \mathbb{N}^2 : (3 + \widehat{s} - \widehat{\gamma})\alpha_1 + (1 + \bar{s})\alpha_2 \leq L \}$$



Method	$\bar{s} = 1, \hat{\gamma} = 1$	$\bar{s} = 1, \hat{\gamma} = 2$	$\bar{s} = 2, \hat{\gamma} = 1$	$\bar{s} = 2, \hat{\gamma} = 2$
MC (Section 3.1)	(3, 0)	(4, 0)	(3, 0)	(4, 0)
MLMC (Section 3.2.1)	(2, 2)	(3, 2)	(2, 0)	(3, 0)
MLMC (Section 3.2.2)	(3, 0)	(3, 2)	(3, 0)	(3, 2)
MLMC (Section 3.2.3)	(2, 2)	(3, 0)	(2, 2)	(3, 0)
MIMC (Section 3.3)	(2, 2)	(2, 4)	(2, 0)	(2, 2)

Table 1

**The work complexity of the different methods presented in this work in common situations, encoded as  $(a, b)$  to represent  $\mathcal{O}(\text{TOL}^a(\log(\text{TOL}^{-1}))^b)$ . When appropriate, we use the partitioning estimator (i.e.,  $\hat{s} = 2$ ). In general, MIMC has always the best complexity. However, when  $\hat{\gamma} = 1$  MIMC does not offer an advantage over an appropriate MLMC method.**

and the optimal computational complexity of MIMC is  $\mathcal{O}(\text{TOL}^{-2+2\max(0,\zeta)} \log(\text{TOL}^{-1})^{\mathfrak{p}})$ , where

$$\begin{aligned}\zeta &= \min\left(\frac{\hat{s} + 1 - \hat{\gamma}}{2}, \frac{\bar{s} - 1}{2}\right), \\ \xi &= \max\left(\frac{1 - \hat{s}}{\hat{\gamma}}, 2 - \bar{s}\right) \geq 0, \\ \mathfrak{p} &= \begin{cases} 0 & \zeta < 0 \\ 2\mathfrak{z} & \zeta = 0 \\ 2(\mathfrak{z} - 1)(\zeta + 1) & \zeta > 0 \text{ and } \xi > 0 \\ 1 + 2(\mathfrak{z} - 1)(\zeta + 1) & \zeta > 0 \text{ and } \xi = 0 \end{cases} \\ \text{and } \mathfrak{z} &= \begin{cases} 1 & \hat{s} + 1 - \hat{\gamma} \neq \bar{s} - 1 \\ 2 & \hat{s} + 1 - \hat{\gamma} = \bar{s} - 1. \end{cases}\end{aligned}$$

**Kuramoto Example.** Here again, we use a naive calculation method of  $\phi_P^N$  (yielding  $\hat{\gamma} = 2$ ) and the partitioning sampler (yielding  $\hat{s} = 1$ ). Finally the constant diffusion coefficient gives  $\bar{s} = 2$ . Hence,  $\zeta = 0$ ,  $\mathfrak{z} = 1$  and  $\text{Work}[\mathcal{A}_{\text{MIMC}}] = \mathcal{O}(\text{TOL}^{-2} \log(\text{TOL}^{-1})^2)$ . See also Table 1 for the work complexities for different common values of  $\bar{s}$  and  $\hat{\gamma}$ .

## 4 Numerical Example

In this section we provide numerical evidence of the assumptions and work complexities that were made in the Section 3. This section also verifies that the constants of the work complexity (which are not tracked) are not significant for reasonable error tolerances. The results in this section were obtained using the `mimc` software library [17].

We compare the MLMC [13] method in the setting that was presented in Section 3.2.3 and the MIMC [18] method that was presented in Section 3.3, using the corresponding algorithms that were outlined in their original work. These particular settings provide a straightforward way to check the bias of the estimator by checking the absolute value of the level differences in MLMC or the multi-index differences in MIMC. On the other hand, checking the bias in the settings outlined in Sections 3.1, 3.2.1 and 3.2.2 is not as straightforward since determining the number of times steps and/or the number of particles estimator is not trivial. This makes a fair numerical comparison difficult. As such, we only verify the assumptions that are required for these methods.

In the results outlined below, we focus on the Kuramoto example in (3), with the following choices:  $\sigma = 0.4$ ,  $T = 1$ ,  $x_p^0 \sim \mathcal{N}(0, 0.2)$  and  $\vartheta_p \sim \mathcal{U}(-0.2, 0.2)$  for all  $p$ . We also make the choice  $P_\ell = 5 \times 2^\ell$  and  $N_\ell = 4 \times 2^\ell$  for MLMC and  $P_{\alpha_1} = 5 \times 2^{\alpha_1}$  and  $N_{\alpha_2} = 4 \times 2^{\alpha_2}$  for MIMC.

Figure 1 shows the absolute expectation and variance of the level differences for the different MLMC settings that were outlined in Section 3.2. These figures verify Assumptions (P1), (P2) and (MLMC1)–(MLMC3) for the values  $\bar{s} = 2$  and  $\hat{s} = 0$  for the  $\bar{\varphi}$  sampler in (8) or the value  $\hat{s} = 1$

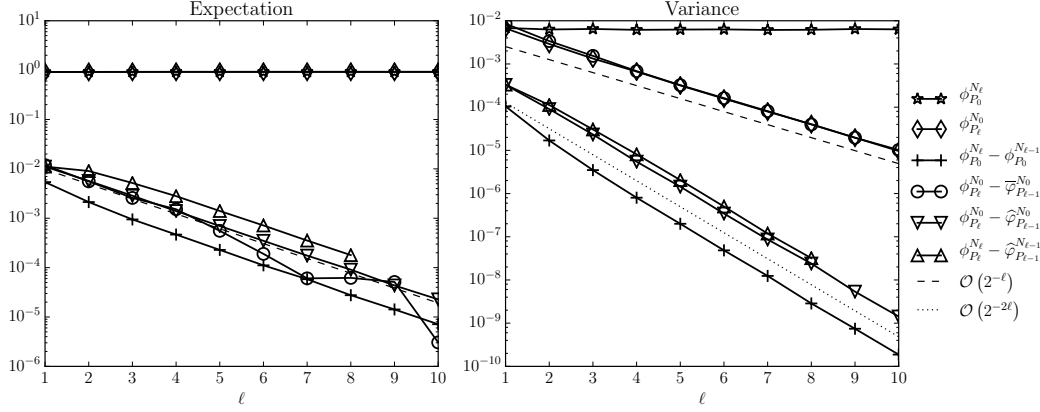


Figure 1: For the choice  $P_\ell = 5 \times 2^\ell$  and  $N_\ell = 4 \times 2^\ell$ , this plot shows, for (3), numerical evidence for Assumption (P1) (left) and Assumptions (P2), (MLMC1)–(MLMC3) (right). From the right plot, we can confirm that  $\bar{s} = 1$ . We can also deduce that using the  $\bar{\varphi}$  sampler in (8) yields  $\hat{s} = 0$  (i.e., no variance reduction compared to  $\text{Var}[\phi_{P_\ell}^{N_\ell}]$ ) while using the  $\hat{\varphi}$  sampler in (9) yields  $\hat{s} = 1$ .

for the  $\hat{\varphi}$  sampler in (9). For the same parameter values, Figure 2 provides numerical evidence for Assumptions (MIMC1) and (MIMC2).

Figure 3-left shows the exact errors of both MLMC and MIMC versus the prescribed tolerance. This plot shows that both methods estimate the quantity of interest up to the same error tolerance. While Figure 3-right show that our assumption in Section 2 of the asymptotic normality of these estimators is well founded. The comparison of the work complexity in Figure 4 is thus fair. The latter figure shows the performance improvement of MIMC over MLMC and shows that the complexity rates that we derived in this work are reasonably accurate.

## 5 Conclusions

This work has shown both theoretically and numerically under certain assumptions, that could be verified numerically, the improvement of MIMC over MLMC when used to approximate a quantity of interest computed on a particle system as the number of particles goes to infinity. The application to other particle systems (or equivalently other McKean-Vlasov SDEs) is straightforward and similar improvements are expected. The same machinery was also suggested for approximating nested expectations in [14] and the analysis here applies to that setting as well. Moreover, the same machinery, i.e., multi-index structure with respect to time steps and number of particles coupled with a partitioning estimator, could be used to create control variates to reduce the computational cost of approximating quantities of interest on stochastic particle systems with a finite number of particles.

Future work includes analyzing the optimal level separation parameters,  $\hat{\beta}$  and  $\bar{\beta}$ , and the behavior of the tolerance splitting parameter,  $\theta$ . Another direction could be applying the MIMC method to higher-dimensional particle systems such as the crowd model in [16]. On the theoretical side, the next step is to prove the assumptions that were postulated in this work for certain classes of particle systems, namely: The bias assumption (P1), the variance assumption (P2), the second order convergence of the variance of the partitioning estimator (MLMC2) with  $\hat{s} = 2$  and the MIMC rates for mixed differences (MIMC1) and (MIMC2). Finally, the same methodology with a partitioning estimator could be applied to other multi-index samplers such as Multi-index Quasi Monte Carlo (MIQMC) [24].

## Acknowledgments

R. Tempone is a member of the KAUST Strategic Research Initiative, Center for Uncertainty Quantification in Computational Sciences and Engineering. R. Tempone received support from the

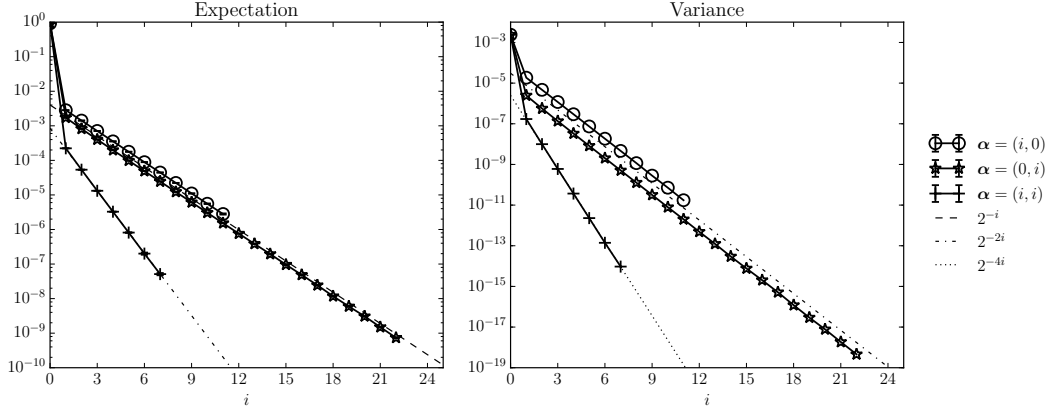


Figure 2: This figure provide numerical evidence for **(MIMC1)** (*left*) and **(MIMC2)** (*right*) for (3) when using the Euler-Maruyama scheme for time discretization (yielding  $\bar{s} = 2$ ) and the partitioning sample of particle systems (yielding  $\hat{s} = 2$ ). Here, the number of particles is taken to be  $P_{\alpha_1} = 5 \times 2^{\alpha_2}$ , while the number of time steps is taken to be  $N_{\alpha_2} = 4 \times 2^{\alpha_2}$ . When considering a mixed difference (i.e,  $\alpha = (i, i)$ ), a higher rate of convergence is observed.

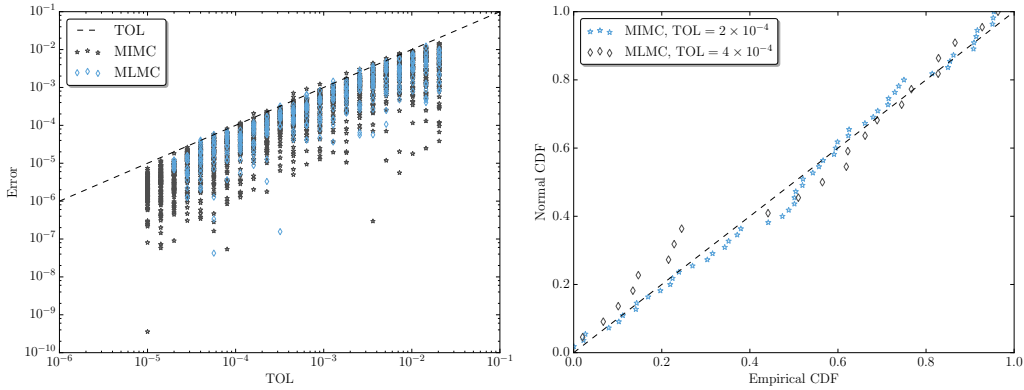


Figure 3: In this plot, each marker represents a separate run of the MLMC or MIMC estimators (as detailed in Sections 3.2.3 and 3.3, respectively) when applied to (3). *Left*: the exact errors of the estimators. This plot shows that, up to the prescribed 95% confidence level, both methods approximate the quantity of interest to the same required tolerance, TOL. *Right*: A QQ plot of the cumulative distribution function (CDF) of the value of both estimators with with  $\text{TOL} = 8 \times 10^{-5}$ , shifted by their mean and scaled by their standard deviation showing that both estimators, when appropriately shifted and scaled, are well approximated by a standard normal random variable.

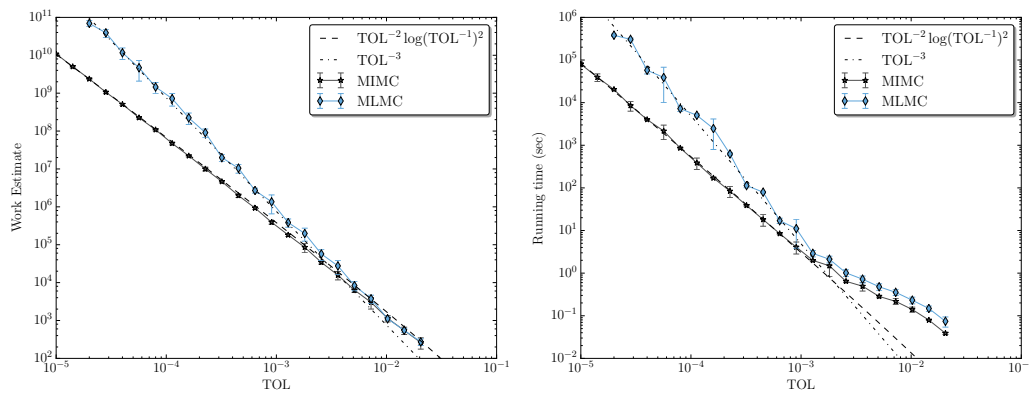


Figure 4: Work estimate (*left*) and running time (in seconds, *right*) of MLMC (detailed in Section 3.2.3) and MIMC (detailed in Section 3.3) when applied to (3). For sufficiently small tolerances, the running time closely follows the predicted theoretical rates (also plotted) and shows the performance improvement of MIMC.

KAUST CRG3 Award Ref: 2281 and the KAUST CRG4 Award Ref:2584.

## References

- [1] ACEBRÓN, J. A., BONILLA, L. L., VICENTE, C. J. P., RITORT, F., AND SPIGLER, R. The kuramoto model: A simple paradigm for synchronization phenomena. *Reviews of modern physics* 77, 1 (2005), 137.
- [2] BOLLEY, F., CANIZO, J. A., AND CARRILLO, J. A. Stochastic mean-field limit: non-Lipschitz forces and swarming. *Mathematical Models and Methods in Applied Sciences* 21, 11 (2011), 2179–2210.
- [3] BOSSY, M., AND TALAY, D. A stochastic particle method for the McKean-Vlasov and the Burgers equation. *Mathematics of Computation of the American Mathematical Society* 66, 217 (1997), 157–192.
- [4] BOSSY, M., TALAY, D., ET AL. Convergence rate for the approximation of the limit law of weakly interacting particles: application to the burgers equation. *The Annals of Applied Probability* 6, 3 (1996), 818–861.
- [5] BUJOK, K., HAMBLY, B., AND REISINGER, C. Multilevel simulation of functionals of Bernoulli random variables with application to basket credit derivatives. *Methodology and Computing in Applied Probability* (2013), 1–26.
- [6] CLIFFE, K., GILES, M., SCHEICHL, R., AND TECKENTRUP, A. Multilevel Monte Carlo methods and applications to elliptic pdes with random coefficients. *Computing and Visualization in Science* 14, 1 (2011), 3–15.
- [7] COLLIER, N., HAJI-ALI, A.-L., NOBILE, F., VON SCHWERIN, E., AND TEMPONE, R. A continuation multilevel Monte Carlo algorithm. *BIT Numerical Mathematics* 55, 2 (2015), 399–432.
- [8] DOBRAMYSL, U., RÜDIGER, S., AND ERBAN, R. Particle-based multiscale modeling of intracellular calcium dynamics. *arXiv preprint arXiv:1504.00146* (2015).
- [9] ERBAN, R., AND HASKOVEC, J. From individual to collective behaviour of coupled velocity jump processes: a locust example. *arXiv preprint arXiv:1104.2584* (2011).
- [10] ERBAN, R., HASKOVEC, J., AND SUN, Y. On Cucker-Smale model with noise and delay. *arXiv preprint arXiv:1507.04432* (2015).

- [11] GÄRTNER, J. On the McKean-Vlasov limit for interacting diffusions. *Mathematische Nachrichten* 137, 1 (1988), 197–248.
- [12] GILES, M. B. Improved Multilevel Monte Carlo convergence using the Milstein scheme. In *Monte Carlo and Quasi-Monte Carlo Methods 2006*, A. Keller, S. Heinrich, and H. Niederreiter, Eds. Springer Berlin Heidelberg, 2008, pp. 343–358.
- [13] GILES, M. B. Multilevel Monte Carlo path simulation. *Operations Research* 56, 3 (2008), 607–617.
- [14] GILES, M. B. Multilevel Monte Carlo methods. *Acta Numerica* 24 (2015), 259–328.
- [15] GILES, M. B., AND SZPRUCH, L. Antithetic multilevel Monte Carlo estimation for multi-dimensional SDEs without Lévy area simulation. *The Annals of Applied Probability* 24, 4 (Aug. 2014), 1585–1620.
- [16] HAJI-ALI, A.-L. *Pedestrian Flow in the Mean-field Limit*. PhD thesis, King Abdullah University of Science and Technology, 2012.
- [17] HAJI-ALI, A.-L. mimclib. <https://github.com/StochasticNumerics/mimclib>, 2016.
- [18] HAJI-ALI, A.-L., NOBILE, F., AND TEMPONE, R. Multi-index Monte Carlo: when sparsity meets sampling. *Numerische Mathematik* 132 (2015), 767–806.
- [19] HAJI-ALI, A.-L., NOBILE, F., VON SCHWERIN, E., AND TEMPONE, R. Optimization of mesh hierarchies in multilevel Monte Carlo samplers. *Stochastic Partial Differential Equations: Analysis and Computations* 4 (2015), 76–112.
- [20] HEINRICH, S. Multilevel Monte Carlo methods. In *Large-Scale Scientific Computing*, vol. 2179 of *Lecture Notes in Computer Science*. Springer Berlin Heidelberg, 2001, pp. 58–67.
- [21] HELBING, D., AND MOLNAR, P. Social force model for pedestrian dynamics. *Physical review E* 51, 5 (1995), 4282.
- [22] KLOEDEN, P., AND PLATEN, E. *Numerical Solution of Stochastic Differential Equations* Springer. 1992.
- [23] RICKETSON, L. A multilevel Monte Carlo method for a class of McKean-Vlasov processes. *arXiv preprint arXiv:1508.02299* (2015).
- [24] ROBBE, P., NUYENS, D., AND VANDEWALLE, S. A multi-index quasi-monte carlo algorithm for lognormal diffusion problems. *arXiv preprint arXiv:1608.03157* (2016).
- [25] ROSIN, M., RICKETSON, L., DIMITS, A., CAFLISCH, R., AND COHEN, B. Multilevel Monte Carlo simulation of coulomb collisions. *Journal of Computational Physics* 274 (2014), 140–157.
- [26] SZNITMAN, A.-S. Topics in propagation of chaos. In *Ecole d’été de probabilités de Saint-Flour XIX1989*. Springer, 1991, pp. 165–251.